JOURNAL OF MATERIALS SCIENCE **36** (2001) 3565–3571

Microstructure and electrical properties of perovskite (Pb, La)TiO_3 thin film deposited at low temperature by the polymeric precursor method

F. M. PONTES, J. H. G. RANGEL, E. R. LEITE, E. LONGO
Department of Chemistry, Federal University of São Carlos-UFSCar, Caixa Postal 676, 13560-905 São Carlos, SP, Brazil
E-mail: liec@power.ufscar.br

J. A. VARELA
Institute of Chemistry, UNESP, Caixa Postal 355, 14801-970 Araraquara, SP, Brazil

E. B. ARAÚJO, J. A. EIRAS
Department of Physics, Federal University of São Carlos-UFSCar, Caixa Postal 676, 13560-905 São Carlos, SP, Brazil

High-quality (Pb, La)TiO_3 ferroelectric thin films were successfully prepared on a Pt(111)/Ti/SiO_2/Si(100) substrate for the first time by spin coating, using the polymeric precursor method. The X-ray diffraction patterns show that the films are polycrystalline in nature. This method allows for low temperature (500° C) synthesis, a high quality microstructure and superior dielectric properties. The effects on the microstructure and electrical properties were studied by changing the La content. The films annealed at 500°C have a single perovskite phase with only a tetragonal or pseudocubic structure. As the La content is increased, the dielectric constant of PLT thin films increases from 570 up to 1138 at room temperature. The *C-V* and *P-E* characteristics of perovskite thin films prepared at a low temperature show normal ferroelectric behavior, representing the ferroelectric switching property. The remanent polarization and coercive field of the films deposited decreased due to the transformation from the ferroelectric to the paraelectric phase with an increased La content.

1. Introduction

Much attention has recently focused on ferroelectric thin films because of their possible applications in non-volatile random access memory (NVRAM) devices, pyroelectric infrared (IR) sensors, and dynamic random access memories (DRAM) [1–5]. Among the ferroelectric perovskite oxides (ABO_3), $Pb_{1-x}La_xTiO_3$ (abbreviated as PLT) is a perovskite-type ferroelectric ceramic in which La^{+3} ions are substituted for Pb^{+2} ions. In bulk PLT, it is known that the capacitance increases and the remanent polarization decreases as the La content [6] is increased. The electrical properties of PLT thin films are also known to be dependent on the La content. An appropriate control of compositions within this system allows for a wide range of dielectric and ferroelectric properties. Moreover, since PLT films have reasonable coercive fields and switchable remanent polarization according to the La doping concentration, they may serve as an alternative material for PZT in NVRAM applications [7, 8].

PLT thin films have been produced mainly by sputtering [9–11], multiple cathode sputtering [12], sol-gel [13–15], chemical vapor deposition [16], and metal organic chemical vapor deposition (MOCVD) [17]. While high-quality ferroelectric thin films have been prepared using both approaches (physical and chemical methods), solution deposition methods offer a number of significant advantages over physical deposition methods. Most notably, solution deposition allows not only for close control of chemical composition and stoichiometry but also for uniform incorporation of minor dopants. Moreover, solution deposition is relatively fast, inexpensive, and compatible with standard semiconductor processing procedures. Among the several chemical solution deposition methods, the sol-gel technique has been widely used for the production of PLT thin films with various compositions. However, some of the disadvantages of many of the available metal alkoxides in methoxyethanol solvent for thin film applications are their extreme reactivity toward atmospheric moisture and the limited crack-free thickness of thin film.

In this work, the chemical solution deposition method, known as the "polymeric precursor method" (PPM) [18–22], has been studied for the first time for the production of PLT thin films containing 0, 13 and 27 mol% concentration of lanthanum. Lee *et al*. [23] recently reported the preparation of $BaTiO_3$ thin films by

polymeric precursor method. This method offers advantages over the sol-gel method, mainly because it uses water as the solvent and presents high stability toward atmospheric moisture. In this study, the effects of La doping are described using "polymeric precursor method" on the surface morphology and electrical properties. The frequency dependence of the dielectric constant, *P-E* hysteresis loop, and capacitance-voltage (*C-V*) characteristics for PLT thin film capacitors with metal-ferroelectric-metal configuration are also studied.

TABLE I Raw materials used in the PLT synthesis

Material	Source	Purity
Lead (II) acetate trihydrate ($Pb(CH_3COO)_2{\cdot}3H_2O$)	Aldrich Chemical	99.9%
Lanthanum oxide (La_2O_3)	Riedel de Haen A. G.	99.999%
Titanium (IV) isopropoxide ($Ti(OCH(CH_3)_2]_4$)	Riedel de Haen A. G.	99.999%
Ethylene glycol	E. Merck	99.9%
Citric acid	E. Merck	99.9%

2. Experimental procedure

Lead (II) acetate trihydrate ($Pb(CH_3COO)_2{\cdot}3H_2O$), Lanthanum oxide ($La_2O_3$) and Titanium (IV) isopropoxide ($Ti(OCH(CH_3)_2]_4$ were used as starting materials. Ethylene glycol and citric acid were used as polymerization/complexation agents for the process. Ammonium hydroxide was used to adjust the pH and to prevent lead citrate precipitation. The procedure for the preparation of a PLT sol is outlined in the flow chart in Fig. 1. The raw materials used for PLT synthesis, as well as the sources, are described in Table I.

Following the flow chart shown in Fig. 1, titanium citrates were formed by the dissolution of titanium IV isopropoxide in a water solution of citric acid (60°–70°C). After homogenization of the Ti-citrate solution, at a concentration of (0.0084 mol/L), a stoichiometric amount of ($Pb(CH_3COO)_2{\cdot}3H_2O$) was dissolved in water and soon thereafter added to the Ti-Citrate solution while it was stirred slowly until a clear solution was obtained. In the case of the 13 and 27 mol% of lanthanum solution, La_2O_3 was first dissolved in a nitric acid solution (10/90) and was later also added gradually to the Pb-Ti-citrate solution. To achieve total dissolution of the cations (Pb and La), ammonium hydroxide was added drop by drop until the pH reached 7-8. The complete dissolution of the salts resulted in a clear solution.

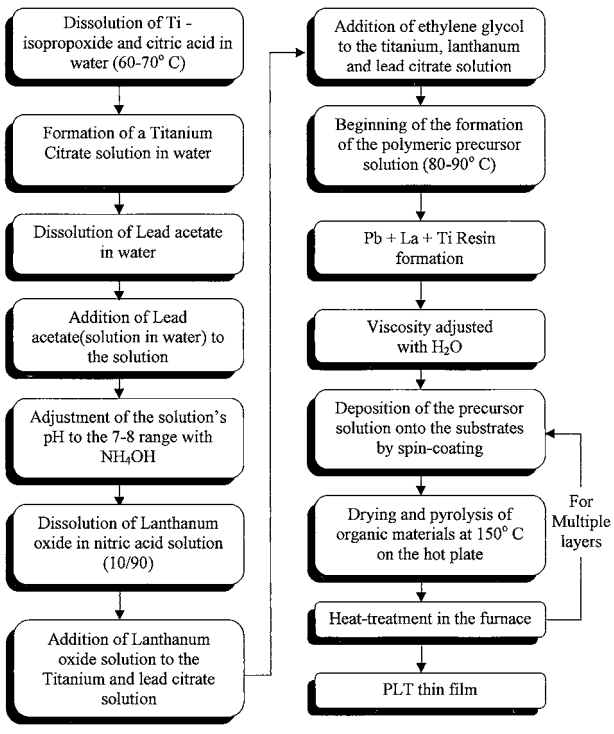

Figure 1 Flow-chart illustrating the procedure for the preparation of PLT solution and film production.

After homogenization of the solution containing the Pb and La cations, ethylene glycol was added to promote mixed citrate polymerization by polyesterification reaction. With continued heating at 80–90 °C, the solution became more viscous, without any visible phase separation. The molar ratio among the Lead-lanthanum and titanium cations was 1:1, the citric acid/metal molar ratio was fixed at 1.00, and the citric acid/ethylene glycol ratio was fixed at 60/40 (mass ratio). The viscosity of the deposition solution was adjusted at 30 mPa·s by controlling the water content.

Pt(111)/Ti/SiO_2/Si(100) wafers were used as substrates. The substrate was spin-coated by dropping a small amount of the polymeric precursor solution onto it. Rotation speed and spin time were fixed at 4800 rpm and 20 s, respectively. After deposition, each layer was dried at 150°C on a hot plate for 20 min to remove residual solvents.

The heat treatment was carried out in two stages: initial heating at 350°C for 4 h in oxygen at a heating rate of 2°C/min to pyrolyze the organic materials, followed soon thereafter by heating at 500°C for 4 h in oxygen to crystallize them. Film thickness was controlled by adjusting the number of layers and each layer was pyrolyzed at 350°C and crystallized at 500°C before the next layer was coated. Four layers were used in this study.

The PLT films were characterized in terms of structure using X-ray diffraction (XRD) (Fe Kα radiation). The diffraction patterns were recorded on a Siemens D5000 machine in a θ–2θ configuration, using a graphite monochromator. Microstructural characterization was performed by scanning electron microscopy (SEM) (Zeiss, DSM940A). The film thickness was measured by a thin film cross-section analysis made by SEM. Atomic force microscopy (AFM) was used to obtain a 3D-image reconstruction of the sample surface. These images allow for an accurate analysis of the sample surface and the quantification of very important parameters such as roughness and grain size. A Digital Instruments Multi-Mode Nanoscope IIIa was used.

To carry out the electrical measurements, 0.3 mm diameter Au electrodes were deposited by sputtering through a designed mask onto the film surfaces (area of 1 cm × 1 cm) to form metal-ferroelectric-metal

capacitors (MFM). The dielectric properties were measured as a function of frequency using a Hewlett-Packard (4194A) impedance/gain phase analyzer.

The capacitance-voltage characteristic was measured for MFM configuration using a small AC signal of 10 mV at 100 kHz. The signal was applied across the sample, while the DC electric field was swept from positive bias to negative bias and back again to positive bias (C-V curves). Dielectric constant and dissipation factor values were measured at a frequency range of 100 Hz–10 MHz in a range of 280–380 nm thick films. Hysteresis loop measurements were carried out on the films with a Radiant Technology RT6000HVS. Hysteresis loops were traced by means of the program *Charge* included in the software of the RT6000HVS in a virtual ground mode test device. All the measurements were taken at room temperature.

3. Results and discussion

3.1. Crystallographic structure

Fig. 2 shows the diffraction patterns of the PLT films with various La contents grown on Pt/Ti/SiO2/Si substrates after heat treatment at 500°C for 4 h. A polycrystalline thin film can be observed in the pattern. The PLT films have a stable perovskite phase, and no other phases were observed. The film without La doping, i.e., $PbTiO_3$ (PLT(0) abbreviated), has (001)/(100) and (002)/(200) peaks which can be distinguished from each other. Interestingly, a peak splitting of (001)/(001) was observed for the peaks from the PLT (13) films. The splitting that was observed indicates that these films present a c/a ratio close to 1.00 (pseudocubic structure). The tetragonality (c/a ratio) of the PLT films decreased with increasing La content. These results suggest that the phase transformation from a tetragonal to a cubic perovskite structure will occur as the La content increases at room temperature. The lattice constants calculated for PLT(0), PLT (13) and PLT (27) were $a = 0.3915$ nm and $c = 0.4105$ nm, $a = 0.3923$ nm $c = 0.4104$ nm, and $a = 0.3926$ nm, respectively. The lattice strain $c/a = 1.048$ (PLT(0)) and $c/a = 1.046$ (PLT(13)) are smaller than $c/a = 1.063$ of the bulk specimen. The values reported here are similar to those reported by Maeda *et al*. [24] and by Lee *et al*. [25].

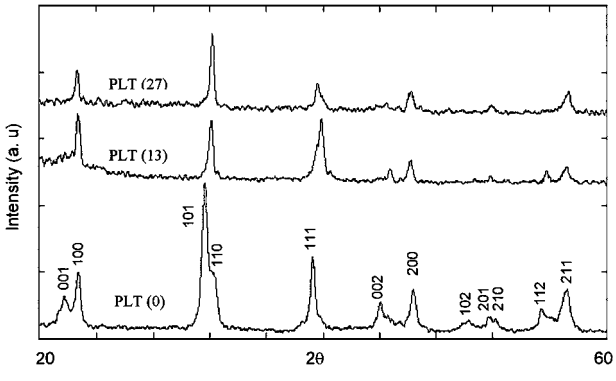

Figure 2 X-ray diffraction patterns of PLT thin films with various La content.

3.2. Surface morphology and microstructure

The microstructural evolution of PLT (0, 13 and 27 mol% La) films deposited on Pt coated silicon substrates and heat treated at 500°C is shown in the two-dimensional AFM images in Fig. 3. AFM imaging was carried out in the contact mode, using a triangular shaped 200-micron long cantilever with a spring constant of 0.06 N/m. The scanning rate varied from 1 to 2 Hz and the applied force from 10 to 50 nN, depending on the sample/tip interactions. The surface roughness (rms) was calculated using the equipment's software routine. As shown in Fig. 3, the surface morphologies of PLT films were characterized as smooth surface, and dense and crack-free microstructure, whose surface microstructure is strongly dependent on the La content. The root mean square surface roughness of the films decreased with increasing La content, changing from 3.6 nm for PLT (0%) to 1.3 nm for PLT (27%) film. These values are an improvement over those reported by Lee *et al*. for PLT thin films obtained by the sol-gel technique.

The average grain in the PLT (0%) film was uniform in size (≅110–120 nm), with a rounded shape. The average grain size for the La doped PT was significantly smaller, consisting of the small grains in PLT (27%) film, round in shape and uniform in size (≅50–60 nm). The behavior observed here is consistent with other results for PLT thin films obtained by other techniques [16, 25]. Film thickness ranged from 280 to 380 nm (SEM analysis) were obtained.

3.3. Electrical properties of PLT thin films deposited at 500°C

The effects of La content on the ferroelectric properties of PLT thin films were investigated studying the frequency influence over the dielectric constant, P-E hysteresis loop, and capacitance-voltage (C-V) characteristics at room temperature.

Fig. 4 shows the dependence of the dielectric constant and dielectric loss in a frequency range of 100 Hz to 10 MHz for the 0, 13, and 27 mol% of La. It can be seen that the dielectric constant increased with the increased La content, varying from 570 for PLT (0 mol% of La) to 1138 for PLT (27 mol% of La) thin films. These values are better than those reported by Lee *et al*. [25] for PLT thin films obtained by the sol-gel technique with an La content close to the films reported in this work. Also, Wang *et al*. [26] reported PLT thin films obtained by the Diol-Based sol-gel process, in which the dielectric constant values were about 50–110 to 900 nm thickness obtained by 4-layers and heated at 700°C, with an La content ranging from 0–20 mol%.

Table II shows some of the results for PLT thin films prepared by other techniques. The dielectric constant is defined as a coefficient of charge variation according to the change of an applied electric field, so that it is dependent on the velocity of dipole movement. Therefore, as the La content increases, the dielectric constant increases. This increase may be explained by the fact that the vacancy concentration increases with increasing La content. Since La ions occupy the Pb

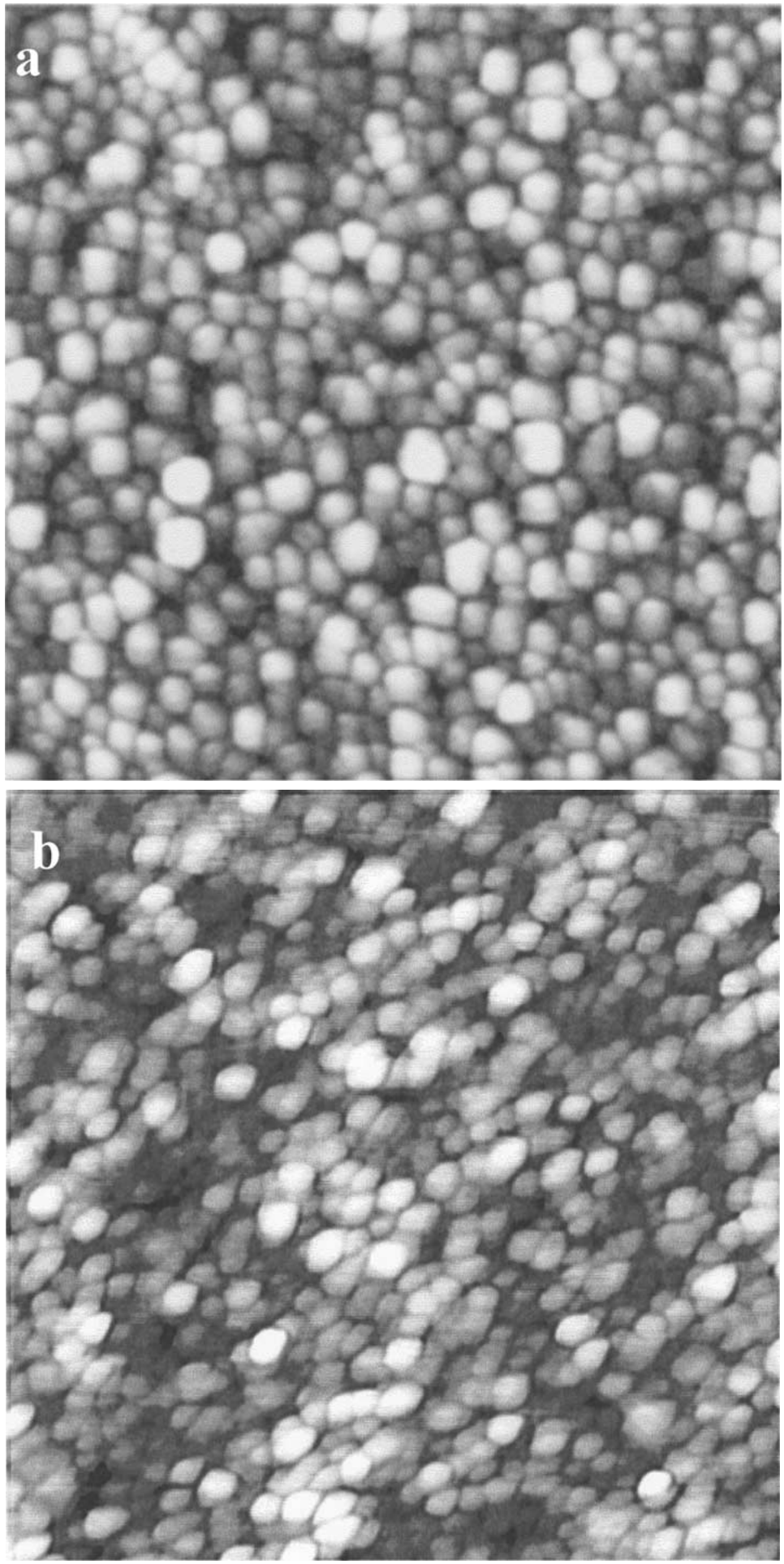

Figure 3 Two-dimensional AFM surface image of PLT thin film annealed at 500°C; a) PLT (0), b) PLT (13), and c) PLT (27) (scan 2 μm × 2 μm) *(Continued)*.

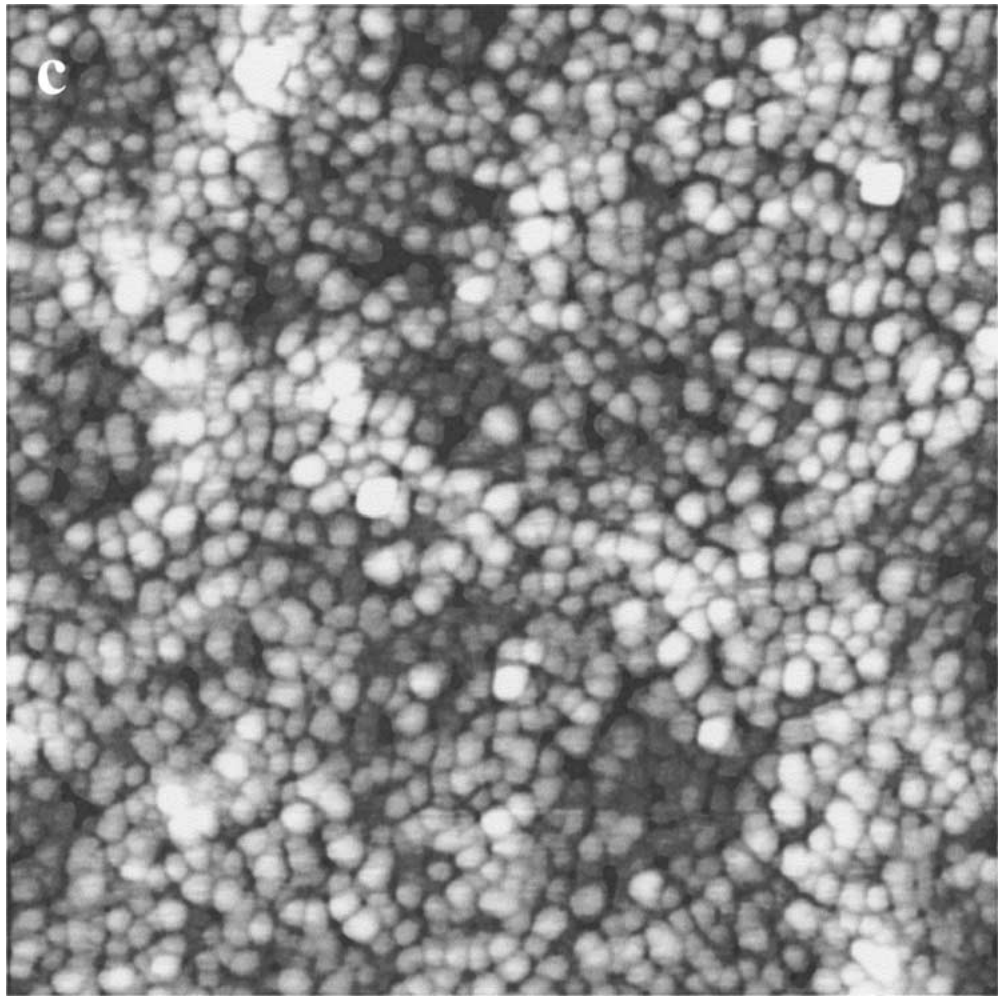

Figure 3 (Continued).

TABLE II Electrical properties of PLT film according to literature

Processing Temp. °C	Composition of La content	Dielectric Constant 100 kHz	Thickness nm	Deposition Method
600	PLT(12)	550	280	Sol-gel [25]
600	PLT(28)	850	280	Sol-gel [25]
600	PLT(0)	150	280	Sol-gel [25]
650	PLT(15)	550	480	Sol-gel [27]
650	PLT(28)	750	480	Sol-gel [27]
540	PLT(17)	246	630	Sputtering [9]
650	PLT(15)	210	1000	Sol-gel [28]
540	PLT(10)	240	1000	MOD [29]
500	PLT(0)	570	380	This study
500	PLT(13)	977	330	This study
500	PLT(27)	1138	280	This study

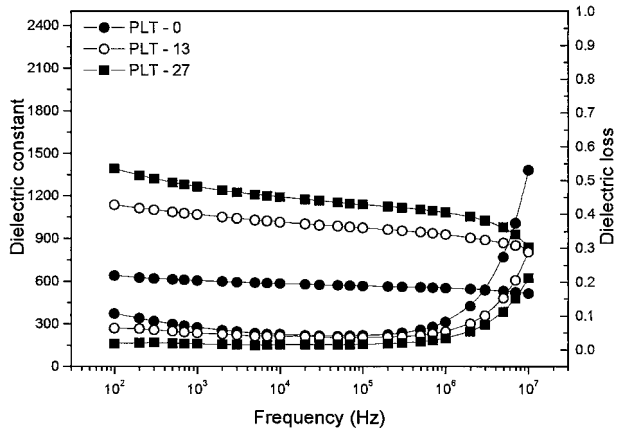

Figure 4 Dielectric constant and dielectric loss as a function of frequency for PLT thin films heat treated at 500°C with various La content.

sites in the lattice, site relations should be maintained; thus, the donor ($La^{\bullet}_{Pb}$) charge must be balanced by an equivalent negative charge of cation vacancies, lead vacancies and/or titanium vacancies (V''_{Pb}, V''''_{Ti}) that will be created in the perovskite lattice. The reactions can be represented as:

$$3TiO_2 + La_2O_3 \rightarrow 2La^{\bullet}_{Pb} + V''_{Pb} + 3Ti_{Ti} + 9O_o \quad (1)$$

$$3TiO_2 + 2La_2O_3 \rightarrow 4La^{\bullet}_{Pb} + 3Ti_{Ti} + V''''_{Ti} + 12O_o \quad (2)$$

As the Pb or Ti vacancy concentration increases, atom transference becomes easier, allowing the domain motions to be produced by a smaller electric field, which results in an increased dielectric constant. This phenomenon is attributed to the increased velocity of dipole movement due the creation of vacancies in PLT films. Another hypothesis for the increase of the dielectric constant is related to the effect of decreasing Curie temperature (T_c) with increasing La concentration, from $T_c \cong 490$°C (PLT(0)) to $T_c \cong 25$° C (PLT(27)). Fig. 5 shows the variation of dielectric constant in PLT thin films with an La content.

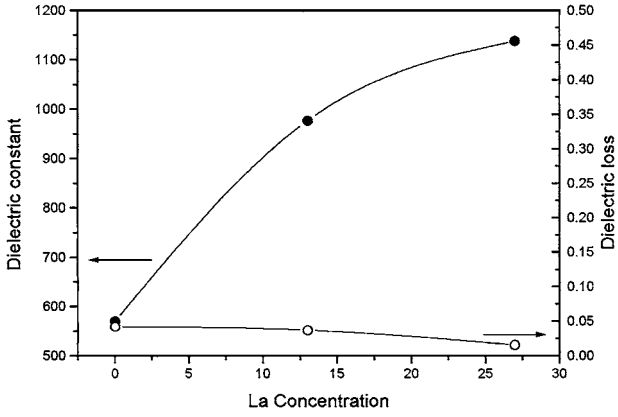

Figure 5 Dielectric constant and dielectric loss of PLT thin films as a function of La content.

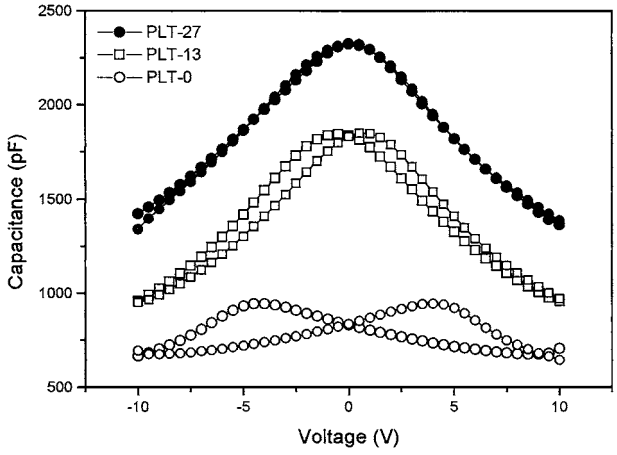

Figure 6 C-V characteristics of the PLT thin films with various La content.

Fig. 6 shows the C-V characteristics of PLT films. The symmetric curves centered at the zero bias axis indicate that the films contain few movable ions or charge accumulation at the film and electrode interface. Substitution of La in the lattice causes a reduction of the tetragonal distortion ($c/a = 1.06$, bulk specimen PT) and decreases the ferroelectric-paraelectric transition temperature (T_c). The film with 27 mol% of La did not present the two peaks, which characterizes spontaneous polarization switching. In other words, the films were in the paraelectric state; therefore, their C-V relations were symmetric and C_{max} (sweep up and sweep down) centered at the zero bias axis.

The dielectric constant calculated from C_{max} ranged from 573 to 1045, which agrees with the calculated value of the dielectric constant versus the frequency curve (Fig. 4).

Fig. 7 shows the P-E hysteresis loops of PLT thin films with 0, 13, and 27 mol% of La at an applied voltage of ± 12 V. For bulk PLT, it is known that, as the La content increases, the ferroelectricity is reduced and that, above La 28%, it becomes paraelectric [30]. The PLT (27 mol% of La) films obtained by the polymeric precursor method in this study also show a very slim hysteresis, with the composition near the ferroelectric-paraelectric phase boundary. The behavior observed here is consistent with that observed by Kang and Yoon [31] for PLT thin films obtained by the

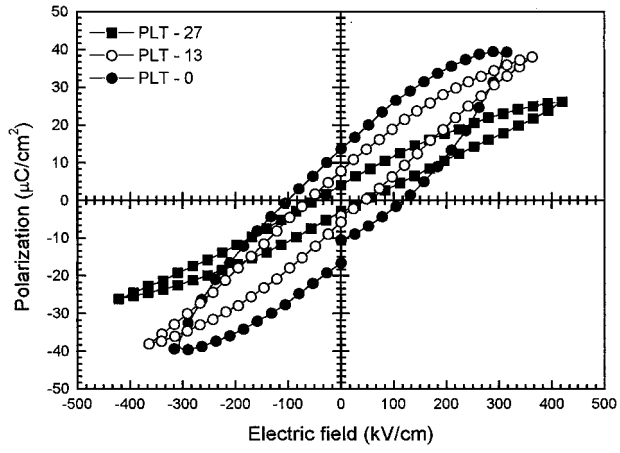

Figure 7 Polarization versus electric field (P-E) curves of the PLT thin films with various La content.

sol-gel technique. The remanent polarization (P_r) and the coercive field (E_c) decreased from 13.62 μC/cm^2 to 3.97 μC/cm^2 and from 120.63 kV/cm to 44.84 kV/cm, respectively, with increased La content in the range of 0 to 27 mol%.

4. Conclusions

Polycrystalline Lanthanum-modified lead titanate thin films with a perovskite structure obtained by the polymeric precursor method were successfully prepared by this method onto Pt/Ti/SiO_2/Si substrate. Homogeneous, crack-free, dense PLT thin films with uniform thickness were produced using the polymeric precursor method, heat-treated in a conventional furnace at 500°C for 4 hour in an oxygen atmosphere. The crystalline structure of the films annealed at 500°C presents a single perovskite phase, changing from the tetragonal to the cubic phase with increasing La content. The microstructure of the films was strongly dependent on the La concentration. The average grain size decreased from 120 to 50 nm, while the surface roughness decreased from 3.6 to 1.3 nm as the La content was increased from 0 to 27% mol La.

The electrical characteristics of the MFM capacitors with PLT thin films showed excellent dielectric and ferroelectric properties. The dielectric constant increased with the increasing La contents of the films, ranging from 570 to 1138. These values are higher and better than the PLT thin films obtained by other techniques, such as sputtering, and sol-gel. The C-V characteristics of MFM capacitors showed a hysteresis loop owing to the ferroelectric switching property. On the other hand, hysteretic behavior decreased with increasing La content, indicating relatively easier switching of the domains with increasing La content. The remanent polarization and coercive field decreased as a result of the phase transformation from ferroelectric to paraelectric with increasing La content ranging from $P_r = 13.62$ μC/cm^2 to 3.97 μC/cm^2 and from $E_c = 120.63$ kV/cm to 44.84 kV/cm.

The results of these studies are very promising, suggesting that PLT thin films obtained by the polymeric precursor method have excellent potential applications

in high dielectric constant capacitors and NVRAM memories.

Acknowledgments

The authors gratefully acknowledge the financial support of the Brazilian financing agencies FAPESP, CNPq, PRONEX and CAPES.

References

1. C. R. CHO, *Mater. Sci. and Engineering* **B64** (1999) 113.
2. A. LI, C. GE, P. LÜ, D. WU, S. XIONG and N. MING, *Mater. Lett.* **31** (1997) 15.
3. B. H. HOERMAN, G. M. FORD, L. D. KAUFMANN and B. W. WESSELS, *Appl. Phys. Lett.* **73**(6) (1998) 2248.
4. T. KAWANO, T. ISOBE, M. SENNA, T. NISHIHARA and J. TANAKA, *Thin Solid Films* **352** (1999) 57.
5. H. H. KIM, S. T. KIM and W. J. LEE, *ibid.* **324** (1998) 101.
6. G. H. HAETLING and C. E. LAND, *J. Amer. Ceram. Soc.* **54** (1971) 1.
7. T. HATA, S. KAWAGOE, W. ZHANG, K. SASAKI and Y. YOSHIOKA, *Vacuum* **51**(4) (1998) 665.
8. J. F. M. CILLESSEN, M. W. J. PRINS and R. M. WOLF, *J. Appl. Phys.* **81**(6) (1997) 2777.
9. H. MAIWA, N. ICHINOSE and K. OKAZAKI, *Jpn. J. Appl. Phys.* **33** (1994) 6227.
10. D. H. LEE, J. S. LEE, S. M. CHO, H. J. NAM, J. H. LEE, J. R. CHOI, K. Y. KIM, S. T. KIM and M. OKUYAMA, *ibid.* **34** (1995) 2453.
11. N. NAGAO, T. TAKEUCHI and K. IIJIMA, *ibid.* **32** (1993) 4056.
12. H. MAIWA, N. ICHINOSE and K. OKAZAKI, *ibid.* **33** (1994) 5240.
13. K. NO, C. G. CHOI, D. S. YOON, T. H. SUNG, Y. C. KIM, I. S. JEONG and W. J. LEE, *ibid.* **35** (1996) 2731.
14. S. J. LEE, M. S. JANG, C. R. CHO, K. Y. KANG and S. K. HAN, *ibid.* **34** (1995) 6133.
15. S. K. DEY, J. J. LEE and P. ALLURI, *ibid.* **34** (1995) 3142.
16. S. W. CHUNG, Y. I. KIM, H. L. PARK and W. J. LEE, *J. Mater. Sci.: Mater. Electronics* **9** (1998) 383.
17. S. S. LEE and H. G. KIM, *Integrated Ferroelectrics* **12** (1996) 83.
18. S. M. ZANETTI, E. R. LEITE, E. LONGO and J. A. VARELA, *J. Mater. Res.* **13**(10) (1998) 2932.
19. *Idem.*, *Mat. Lett.* **31** (1997) 173.
20. C. R. FOSCHINI, E. LONGO, J. A. VARELA and S. B. DESU, *Appl. Phys. Lett.* **75**(4) (1999) 552.
21. V. BOUQUET, E. LONGO, E. R. LEITE and J. A. VARELA, *J. Mater. Res.* **14**(7) (1999) 3115.
22. V. BOUQUET, E. R. LEITE, E. LONGO and J. A. VARELA, *J. Europ. Ceram. Soc.* **19** (1999) 1447.
23. E. J. H. LEE, F. M. PONTES, E. R. LEITE, E. LONGO, J. A. VARELA, E. B. ARAUJO and J. A. EIRAS, *J. Mater. Sci. Lett.* **19** (2000) 1457.
24. M. MAEDA, H. ISHIDA, K. K. K. SOE and I. SIZUKI, *Jpn. J. Appl. Phys.* **32** (1993) 4136.
25. S. J. LEE, K. Y. KANG, S. K. HAN, M. S. JANG, B. G. CHAE, Y. S. YANG and S. H. KIM, *Appl. Phys. Lett.* **72**(3) (1998) 299.
26. C. M. WANG, Y. C. CHEN, M. S. LEE, J. W. WU and C. C. CHIOU, *Jpn. J. Appl. Phys.* **37** (1998) 951.
27. S. J. KANG, D. H. CHANG and Y. S. YOON, *Thin Solid Films* **373** (2000) 53.
28. C. SHI, L. MEIDONG, L. CHURONG, Z. YIKE and J. D. COSTA, *ibid.* **375** (2000) 288.
29. Z.-T SONG, W. REN, L.-Y ZHANG, X. YAO and C. LIN, *ibid.* **353** (1999) 25.
30. G. H. HAETLING and C. E. LAND, *J. Amer. Ceram. Soc.* **54** (1971) 1.
31. S. J. KANG and Y. S. YOON, *Jpn. J. Appl. Phys.* **36**(7A) (1997) 4459.

Received 10 November 1999
and accepted 1 February 2001